Cubic MnSb: epitaxial growth of a predicted room temperature half-metal

James D. Aldous, Christopher W. Burrows, Ana M. Sánchez, Richard Beanland, Ian Maskery, Matthew K. Bradley, Manuel dos Santos Dias, Julie B. Staunton, and Gavin R. Bell*

Department of Physics, University of Warwick, Coventry, UK, CV4 7AL

(Dated: January 26, 2012)

Abstract

Epitaxial films including bulk-like cubic and wurtzite polymorphs of MnSb have been grown by molecular beam epitaxy on GaAs via careful control of the Sb_4/Mn flux ratio. Nonzero-temperature density functional theory was used to predict *ab initio* the half metallicity of the cubic polymorph and compare its spin polarization as a function of reduced magnetization with that of the well known half-metal NiMnSb. In both cases, half-metallicity is lost at a threshold magnetization reduction, corresponding to a temperature $T^* < T_C$. This threshold is far higher for cubic MnSb compared to NiMnSb and corresponds to $T^* > 350$K, making epitaxial cubic MnSb a promising candidate for efficient room temperature spin injection into semiconductors.

PACS numbers: 81.15.Hi, 85.75.-d, 71.15.Dx, 31.15.E-, 72.25.Mk, 68.37.Og, 75.50.Cc

A key goal for the development of semiconductor (SC) spintronics is efficient electrical injection of spin polarized current into a non-magnetic SC structure. Ferromagnetic (FM) materials can be used as a spin source and an ideal material would both provide a fully spin polarized current[1,2] and possess "engineering compatibility" with its SC host. This includes controllable epitaxy and interfaces, and suitability for device processing. Certain half-metallic ferromagnetic (HMF) materials have a theoretical density-of-states (DOS) spin polarization at the Fermi level of $P_{DOS} = 100\%$ due to the presence of a band gap straddling the Fermi energy E_F for one spin channel only[3]. Density functional theory (DFT) has predicted this property in several classes of materials[1–3], including Heusler alloys and transition metal pnictides (TMPs), at temperature $T = 0$K. On this basis, half-metallicity was first envisaged in the ternary Heusler alloy NiMnSb, which has a minority spin gap $E_g \approx 0.5$ eV[4]. However, there is presently no HMF candidate with SC engineering compatibility which clearly maintains $P_{DOS} \approx 100\%$ at room temperature. DFT studies continue to play a key role both in assessing the potential of new HMF materials and in understanding fundamental aspects of the HMF state.

Experimental verification of P_{DOS} is not straightforward and after more than two decades' study, $P_{DOS}(T)$ for NiMnSb is not known. For example, spin polarized photoemission spectroscopy (SPPES) can measure P_{DOS} quite directly, but it is strongly affected by extrinsic effects (e.g. non-stoichiometry, reduced magnetization, reconstruction) at the surface. Threshold SPPES measured $P_{DOS} \leq 50\%$ at $T = 20$K[5], while more recent works measured 40%[6], or 50% at $T = 10$K[7]. Note that spin polarizations in electron transport are not the same as P_{DOS}, and have been inferred from magnetic tunnel junctions (MTJs) or spin light emitting diodes[8], or by Andreev reflection[9]. Useful magnetoresistance has been achieved in MTJs with Heusler alloy contacts[1]. While extrinsic effects can alter spin polarization, such problems can be tackled by improving material quality[10] and epitaxy[11]. It remains crucial to address what are the *intrinsic* limitations on P_{DOS}.

HMF band structures are expected to change as T increases, even well below the Curie temperature T_C[2,12–14]. Theory shows how the DOS in the minority spin gap becomes nonzero as a consequence of the effects of thermally induced spin fluctuations on the electronic structure. In fact, beyond a threshold temperature $T^* < T_C$, the value of P_{DOS} collapses far more rapidly than the reduction of magnetization $M(T)$[12]. This effect may set an intrinsic barrier to the applicability of low-gap HMFs such as NiMnSb to room temperature

spintronics. An HMF material with a larger E_g, as we show later in this letter, can be expected to have a much higher T^*.

The binary TMPs have attracted much recent attention. Materials such as MnAs and CrSb are predicted to be HMF with large E_g in cubic (sphalerite)[15,16] and wurtzite[17] (w-) polymorphs. Here, we predict cubic c-MnSb to be HMF with $E_g = 1.08$ eV, unlike naturally occurring $B8_1$ niccolite structure n-MnSb which is a normal FM metal. Attempts have been made to stabilize cubic TMP polymorphs by high-strain epitaxial growth on common SC substrates, *e.g.* c-CrAs and c-CrSb grown as ultra-thin films on GaAs(001). However, these films revert to their stable non-HMF structures within 2-4 nm thickness[15,18] while X-ray diffraction (XRD) has shown the presence of strained orthorhombic o-CrAs rather than c-CrAs[19]. A recent DFT study of CrAs on GaAs(001) found that bulk-like o-CrAs was favorable for ultra-thin films with just 3 Cr atomic layers, and argued that reported FM hysteresis is due to uncompensated interfacial spins of anti-FM o-CrAs[20]. Highly strained epitaxy does not appear to be a promising route to producing wide-gap HMF thin films of this class and we demonstrate an alternative route in this letter.

We report here the first fully *ab initio* DFT calculations which compare the nonzero-T electronic structure and spin polarization of binary c-MnSb and ternary NiMnSb. These demonstrate that c-MnSb, with its large value of E_g, possesses far more robust half-metallicity than the Heusler alloy. Furthermore, we show for the first time that c-MnSb and w-MnSb can be grown epitaxially on GaAs by careful flux control in molecular beam epitaxy (MBE) without relying on heteroepitaxial strain to stabilize the polymorphs.

We first calculated the $T = 0$ electronic properties of n-, c- and w-MnSb polymorphs using two standard DFT packages[21,22]. (Full details will be given in a longer paper.) Both c-MnSb and w-MnSb are HMF materials with E_g 1.08 eV and 1.15 eV respectively and integer total spin moment $4\mu_B$ at $T = 0$K. The calculated electronic structure of n-MnSb agrees with previous work[23] and shows a weak P_{DOS} of 18%. The change of MnSb structure from n- to c- or w-phases represents true polymorphism since there is a change of bonding from octahedral coordination of Mn by surrounding Sb to tetrahedral coordination of both elements. Conversely, the c- and w- phases are mutual polytypes, differing only in the stacking sequence of (111) or (0001) planes. As expected, they are very close in total energy, calculated respectively at 0.829 and 0.833 eV per formula unit above n-MnSb.

In order to assess the robustness of the half-metallicity to increase in temperature and

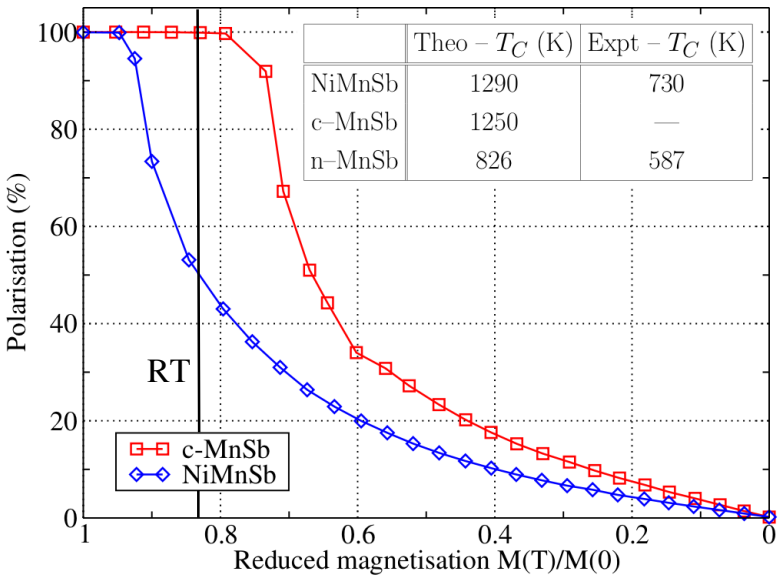

FIG. 1. (color online) Nonzero-T electronic structure theory for MnSb and NiMnSb. The curves show the calculated Fermi level spin polarization P_{DOS} as a function of magnetization reduction for c-MnSb (red squares) and NiMnSb (blue diamonds), while the inset table summarizes calculated T_C values from DLM-DFT. The experimental lattice parameter was assumed for c-MnSb, and the value used for NiMnSb matched that of Ref.[12]. The vertical line labelled RT represents room temperature, assuming the experimental T_C of NiMnSb for both materials.

to estimate T^* we have extended the modelling of the c-MnSb and n-MnSb polymorphs to nonzero-temperature DFT using the disordered local moment (DLM) theory[24,25]. The theory includes the effects of thermally induced spin fluctuations on the underlying electronic structure, which must destroy the long-range magnetic order and the overall spin polarization of the electronic states at $T \geq T_C$. The DLM-DFT approach associates a local spin polarization axis $\hat{e}_i$ or local moment with each lattice site, i. These axes vary slowly on the timescale of the electronic motions, affecting the nature and extent of the spin polarization of the electronic structure and being self-consistently maintained. Thermally-induced disorder in the orientations of the local moments is treated using a mean-field scheme, based on the coherent potential approximation[26,27]. A generalisation of DFT is used to give an energy for a given orientational configuration of the local moments, $\{\hat{e}_i\}$,i.e. $\Omega\{\hat{e}_i\}$. By taking ensemble averages over the local moments' orientational configurations with each configuration given a probability $P\{\hat{e}_i\} = \exp(-\beta\Omega\{\hat{e}_i\}/k_BT)/Z$, where Z is the partition function,[24,28,29] we are

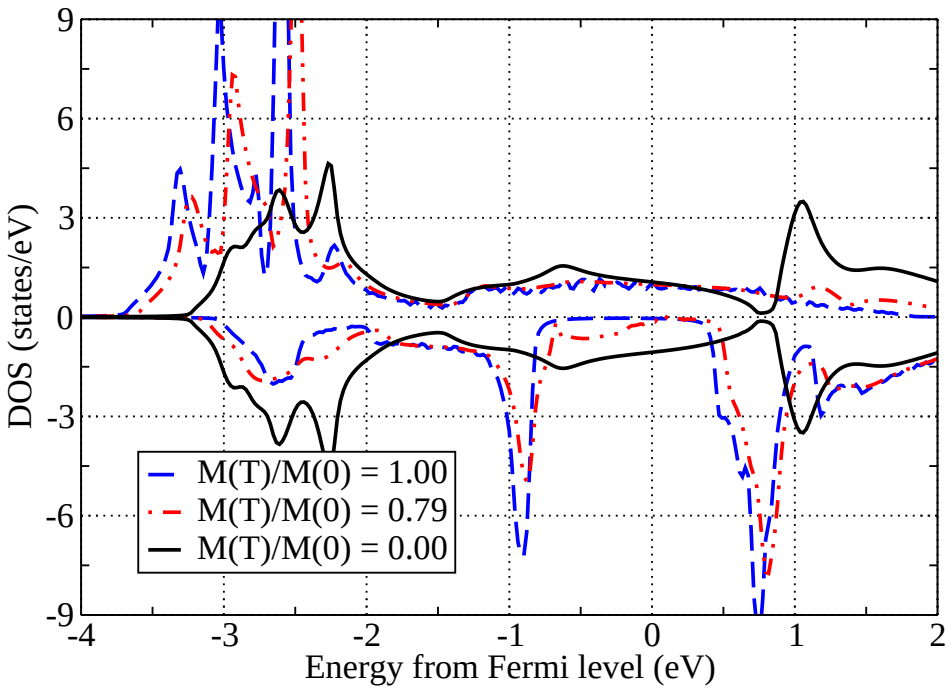

FIG. 2. (color online) Spin-polarized DOS for c-MnSb at different magnetizations $M(T)$ calculated by DLM-DFT at the experimental lattice parameter. The three curves correspond to $T = 0$K (blue dash), $T = T^*$ (red dash-dot) and $T = T_C$ (black solid line): the upper panel shows majority spin DOS, the lower minority spin DOS.

able to determine the system's magnetic properties. These are underpinned by spin polarized electronic structure which varies according to the extent of magnetic order, $M(T)$. We can therefore find P_{DOS} versus $(M(T)/M(0))$. DLM-DFT theory also describes *ab initio* the onset and type of magnetic order[24,25] with an estimate of magnetic transition temperatures. Details can be found in refs.[28,29].

Results of our DLM-DFT calculations are summarized in Fig. 1. The inset tabulates the Curie temperatures for n-MnSb and NiMnSb: in each case our calculated T_C is larger than the experimental value as expected from mean field estimates. Other similar calculations[12] for NiMnSb have also somewhat overestimated T_C. In accord with experiment, however, the theory estimates the T_C of NiMnSb to be significantly higher than that of n-MnSb. Our calculated T_C values for NiMnSb and c-MnSb are very similar. That $T_C \gg 300$ K for c-MnSb is promising but, noted above, does not guarantee a high P_{DOS} at room temperature[14]. The behavior of P_{DOS} predicted by DLM-DFT as a function of magnetization reduction, $M(T)/M(0)$ is plotted in Fig.1 for c-MnSb and compared with that of NiMnSb: the hor-

izontal axis is effectively a distorted temperature scale between 0 and T_C. For NiMnSb, P_{DOS} rapidly collapses after just a 5% reduction in magnetization. The same behavior is evident for c-MnSb but in this case P_{DOS} remains at 100% to a much higher magnetization reduction of around 21%. Using DLM-DFT to estimate the magnetization dependence on temperature $M(T)$ we can compare T^* of NiMnSb and c-MnSb. We find that $T^* \approx 0.14 T_C$ for NiMnSb which translates to 100K or 180K depending on whether the experimental or theoretical value of T_C is used. For c-MnSb $T^* \approx 0.48\ T_C$, i.e. $T^* \approx 350$ K or 620 K using the T_C values of NiMnSb and we deduce that the half-metallicity of c-MnSb is robust against thermal spin fluctuations even above room temperature.

This property stems from the large E_g. In c-MnSb the nearest neighbours of each Mn atom are 4 Sb atoms. The local tetrahedral environment enables the t_{2g} states of Mn to hybridize easily with the Sb p-states so that a large bonding-antibonding splitting is set up where the lower-lying bonding states have more p-character whilst the higher antibonding states are more d-like. The gap in between is partly filled by the non-bonding narrow e_g states of the transition metal. At $T = 0$K Mn has a large exchange splitting which causes the bands of the majority and minority spin electrons to be distributed around different energies[30], E_{maj}, E_{min}. The majority spin d-states of the Mn atoms are closer to the Sb p-states and the bonding-antibonding gap is smaller. For the minority spin electrons the Mn d-states are forced higher by the exchange splitting and the gap for this spin channel straddles E_F with the anti-bonding states unfilled.

At a given T and $M(T)$ the overall spin polarization of the electronic structure is given by the average over an ensemble of non-collinear local moment configurations, $\{\hat{e}_i\}$, weighted by $P\{\hat{e}_i\}$[24]. When $M(T)/M(0)$ is slightly less than unity there is a small chance of a spin-polarized electron encountering a local moment not aligned with the overall magnetization direction. This leads to a small "impurity" majority spin DOS close to E_{min} and a small "impurity" minority spin DOS near E_{maj}. As $M(T)/M(0)$ diminishes these features grow so that a signature of the exchange splitting of the electronic structure persists even above T_C which sustains the local moments despite their orientations becoming disordered. These features are illustrated for c-MnSb in Fig. 2. The minority spin gap $E_g = 1.08$ eV appears in the fully magnetized case corresponding to $T = 0$K (blue curve). The exchange splitting between the antibonding t_{2g} states of the majority and minority spin channels is large so that, as the overall magnetization is reduced, impurity states associated with minority spin

electrons appear in the majority spin channel above E_F whilst majority spin impurity states form in the minority spin gap close to the position of the antibonding t_{2g} majority spin band. As M is reduced, these encroach up to the Fermi level and at T^* remove the half-metallicity abruptly. If E_g were smaller this disruption would happen at a lower T^*. This mechanism is shown in the red curve of Fig. 2: the impurity states have just reached E_F at a magnetization reduction of 21%, initiating the collapse of P_{DOS} shown in Fig. 1. Finally, for $T > T_C$ all spin polarization is lost (black curve). The same effects occur for NiMnSb but at a much lower T^*.

The changes to the DOS which occur as T is increased reflect the effect of spin wave disorder on the quasi-particle excitations. Indeed our DLM treatment of essentially transverse magnetic fluctuations can be considered as the static limit of some, as yet undeveloped, dynamical mean field theory of spin fluctuations[31]. There have also been a number of theoretical studies by Katsnelson, Chioncel and co-workers[33] of electron correlation effects beyond what is available from conventional DFT on the electronic structure of putative HMFs. They set up a multi-orbital Hubbard-type model selecting reasonable U and J parameters. Their subsequent many- body theory analysis focusses on specific effects and shows how dynamical electron-electron correlations may introduce non-quasiparticle states into the minority spin gap. These new minority spin DOS features are qualitatively different from those found for the DLM-DFT shown in Fig. 2. It would be interesting to see this analysis carried out for the T-dependence of spin-polarized DOS of c-MnSb, compared with that NiMnSb together with estimates of the T_c's and to find out whether the half-metallicity of c-MnSb is also robust to increase in T within this approach.

These conclusions add strong impetus to the search for cubic TMP thin films stabilized on SC substrates[20]. We have performed MBE growth of MnSb on GaAs and succeeded in stabilizing cubic and wurtzite polymorphs in films tens of nm thick without high epitaxial strain. The MnSb films were grown on ∼10 mm wide GaAs(111) substrates by MBE, without substrate rotation[34]. The substrate temperature T_{sub} was fixed at 695 ± 5 K, and the growth rate was 6 nm min^{-1}. For each growth run the Sb_4/Mn flux ratio J was measured directly by a retractable ionization gauge. Typically, samples were capped with Sb to prevent oxidation[35]. Specimens were prepared for transmission electron microscopy (TEM) using conventional techniques. They were examined using JEOL 2000FX and Tecnai F20 microscopes operating at 200 kV, using bright field and dark field imaging as well as selected

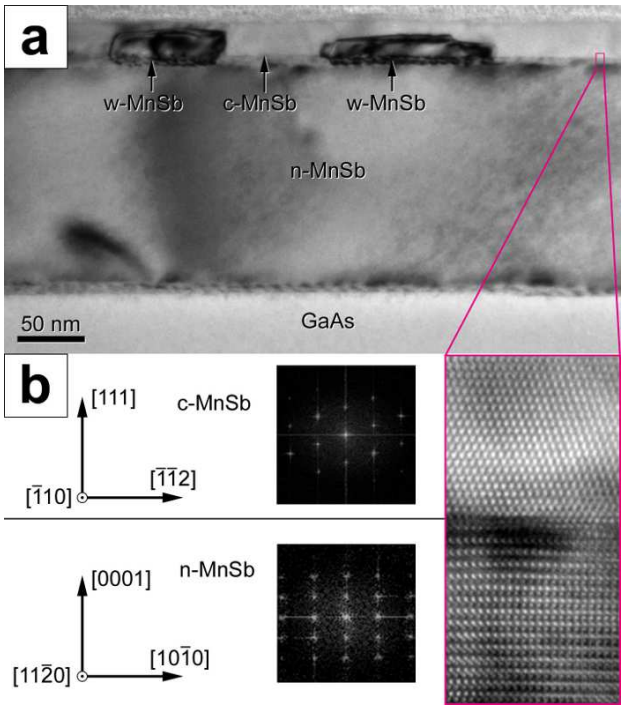

FIG. 3. (color online) TEM data for polymorphic MnSb films on GaAs(111). A typical bright-field image (a) and Fourier transforms from individual regions (b) are labelled with constituent phases, while a high resolution micrograph of the c-MnSb/n-MnSb boundary shows a sharp epitaxial interface.

area diffraction patterns (SADP).

In Fig. 3 we show TEM data from typical polymorphic films. Initially the epilayer grows as n-MnSb, with a high density of misfit dislocations at the n-MnSb/GaAs interface efficiently relaxing the 3.2% in-plane strain within a few nm thickness[34]. However, beyond a certain film thickness (typically 100 nm) a sharp transition to polymorph growth occurs. Careful analysis of the images and SADP reveals that two epitaxial polymorphs of MnSb exist in the upper portion of the films, namely c-MnSb(111) and w-MnSb(0001). Calibrating SADP data to the GaAs substrate gives the following lattice parameters (in Å, uncertainty ±0.5%): n-MnSb a=4.115, c=5.769; w-MnSb a=4.291, c=7.003; c-MnSb a=6.502. For n-MnSb, the lattice parameters conform with results in the literature[23,34], which gives us confidence in the w-MnSb and c-MnSb values, while for w-MnSb, the c/a ratio is almost exactly $1.632 = \sqrt{8/3}$, corresponding to tetrahedral coordination of nearest neighbours. The experimental lattice parameters match the trends from optimized DFT structures. For the substrate and all three polymorphs, the half-crystal symmetries are 3m and in the absence of

translational domains a single epitaxial orientation is predicted[36]. The interface between n-MnSb and the polymorph epilayer is sharp, as shown by the high resolution image in Fig. 3, and maintains the epitaxial relationship. We see no TEM evidence for translational domains and associated double positioning boundaries in the epilayer due to pre-existing GaAs surface steps. The polymorph growth is not influenced by post-growth cycling between 300 K and 700 K and the film structure is stable for many months, provided the samples are protected from oxidation[35]. Films begin to break down on heating to $\geq$ 500 K outside ultra-high vacuum. Furthermore, XRD data (not shown) from as-grown films reveal the presence of w-MnSb and c-MnSb in addition to n-MnSb, and so we can rule out polymorphism as an artefact of TEM specimen preparation. Due to the effusion cell positioning in our MBE chamber, J varies slightly across the sample width. By measuring XRD at different points across the sample we confirmed that c- and w- polymorphs persist uniformly where J lies in the correct range, a distance of around 5 mm. Using standard magetometry, all the films are ferromagnetic up to their breakdown temperature.

On the basis of these observations, we attribute the nucleation of polymorphs to surface processes during MBE growth rather than residual epitaxial strain. In fact, the onset of polymorphism in the films is most strongly correlated with the flux ratio J: careful control of both J and T_{sub} is required to produce c- and w-MnSb. For $J < 5$, the growth rate is Sb-limited while for $J > 8$ the film becomes faceted and non-planar. In the range $6.6 < J < 7.5$, c-MnSb crystallites readily appear in the n-MnSb films. We have not observed polymorphism in films grown at $T_{sub} \leq 675$ K. Surface segregation of Sb leading to a double-layered surface reconstruction with local tetrahedral coordination is a potential explanation for the transition, which requires a layer stacking order change from AbAc (n-) to AaBbCc (c-) or BbCc (w-) in the [111] or [0001] direction. The mechanism for stabilization of these polymorphs is clearly very different from direct epitaxial strain of the SC substrate[15,18–20].

The mechanism of spin polarization reduction in hybridization-gap materials[2,12–14] has been confirmed by the present fully *ab initio* calculations. It is clear that, as well as T_C, E_g is a key parameter in determining the spin polarization. Fully *in situ* investigations of the transition to polymorphic growth should shed more light on the microscopic surface processes leading to the growth transition and enable optimization of the MBE growth. The combination of engineering compatibility and robust spin polarization make c-MnSb highly attractive for spintronics applications. Epitaxial interfacing to a semiconductor remains

a crucial task but the prognosis here is also good. Mollet and Jenkins[37] have calculated the (001) and (111) surface electronic structure of c-MnSb using DFT and found that half-metallicity is preserved for the favored Sb-terminated surfaces. Since this structure is shared with common semiconductors such as GaAs, it is likely that half-metallic interfaces can be formed. In contrast, the preservation of half metallicity at SC interfaces is much less common with ternary Heusler alloys[11]. Interestingly, Jenkins's recent prediction of tilted Dirac cones (similar to those found in graphene and at topological insulator surfaces) in the surface states of NiMnSb[38] is also likely to translate to c-MnSb, since the relevant symmetry of the structures is identical.

We acknowledge support from EPSRC, the Royal Society, Birmingham Science City: Creating and Characterising Next Generation Advanced Materials, and Advantage West Midlands and the European Regional Development Fund, plus a PhD grant SFRH/BD/35738/2007 awarded by FCT Portugal using funding from FSE/POPH.

---

* Electronic mail: gavin.bell@warwick.ac.uk

[1] B. Hillebrands and C. Felser, J. Phys. D: Appl. Phys. **39**, Issue 5 (2006).

[2] M. I. Katsnelson, V. Y. Irkhin, L. Chioncel, A. I. Lichtenstein, and R. A. de Groot, Rev. Mod. Phys. **80**, 315 (2008).

[3] P. Dowben, J. Phys. Condens. Matter **19**, 310301 (2007).

[4] R. A. de Groot, F. M. Mueller, P. G. van Engen, and K. H. J. Buschow, Phys. Rev. B **64**, 060403 (2001).

[5] W. Zhu, B. Sinkovic, E. Vescovo, C. Tanaka and J. S. Moodera, Phys. Rev. Lett. **50**, 2024 (1983).

[6] W. Zhu, B. Sinkovic, E. Vescovo, C. Tanaka and J. S. Moodera, Phys. Rev. B Rapid Comm. **64**, 060403 (2001).

[7] M. Sicot, P. Turban, S. Andrieu, A. Tagliaferri, C. De Nadai, N. B. Brookes, F. Bertran and F. Fortuna J. Mag. Magn. Mater. **303**, 54 (2006).

[8] W. Van Roy, P. Van Dorpe, V. Motsnyi, Z. Liu, G. Borghs and J. De Boeck, phys. stat. sol. **241**, 1470 (2004).

[9] Y. Miyoshi et al., Appl. Phys. Lett. **88**, 142512 (2006).

[10] F. Wang et al., Jpn. J. Appl. Phys. **49**, 025502 (2010).

[11] J. J. Attema, G. A. de Wijs, and R. A. de Groot, J. Phys. D.: Appl. Phys. **39**, 793 (2006).

[12] M. Ležaić, P. Mavropoulos, J. Enkovaara, G. Bihlmayer, and S. Blügel, J. Mater. Sci. **97**, 026404 (2006).

[13] R. Skomski, J. Appl. Phys. **103**, 07D714 (2008).

[14] P. A. Dowben and R. Skomski, J. Appl. Phys. **95**, 7543 (2004).

[15] H. Akinaga, T. Manago, and M. Shirai, Jpn. J. Appl. Phys. **39**, L1118 (2000).

[16] J. E. Pask, L. H. Yang, C. Y. Fong, W. E. Pickett, and S. Dag, Phys. Rev. B **67**, 224420 (2003).

[17] W.-H. Xie, B.-G. Liu, and D. G. Pettifor, Phys. Rev. B **68**, 134407 (2003).

[18] J. H. Zhao, F. Matsukura, E. A. K. Takamura, D. Chiba, and H. Ohno, Appl. Phys. Lett. **79**, 2776 (2001).

[19] V. H. Etgens et al., Phys. Rev. Lett. **92**, 167205 (2004).

[20] S. J. Hashemifar, P. Kratzer, and M. Scheffler, Phys. Rev. B **82**, 214417 (2010).

[21] H. Ebert, D. Ködderitzisch and J. Minár, Rep. Prog. Phys. **74**, 096501 (2011).

[22] S. J. Clark et al., Zeit. Kristallogr. **220**, 567 (2005).

[23] O. Rader et al., Phys. Rev. B. **57**, R689 (1998).

[24] B. L. Gyorffy, A. J. Pindor, J. B. Staunton, G. M. Stocks, and H. Winter, J. Phys. F: Met. Phys. **15**, 1337 (1985).

[25] M. dos Santos Dias, J. B. Staunton, A. Deak, and L. Szunyogh, Phys. Rev. B. **83**, 054435 (2011).

[26] P. Soven, Phys. Rev. **156**, 809 (1967).

[27] G. M. Stocks, W. M. Temmerman and B. L. Gyorffy, Phys. Rev. Lett. **41**, 339 (1978).

[28] J. B. Staunton, B. Gyorffy, G. M. Stocks, and J. Wadsworth, J. Phys. F: Met. Phys. **16**, 1761 (1986).

[29] J. B. Staunton and B. L. Gyorffy, Phys. Rev. Lett. **69**, 371 (1992).

[30] I. Galanakis and P. Mavropoulos, Phys. Rev. B **67**, 104417 (2003).

[31] I. D. Hughes, M. Daene, A. Ernst, W. Hergert, M. Lueders, J. B. Staunton, Z. Szotek and W. M. Temmerman, New J. Phys. **10**, 063010, (2008). (Here we found that the large insulating gaps of the transition metal oxides are unchanged by the loss of magnetic order above T_N.)

[32] L. Chioncel, E. Arrigoni, M. I. Katsnelson and A. I. Lichtenstein, Phys. Rev. Lett. **96**, 137203, (2006).

[33] M. I. Katsnelson, V. Yu. Irkhin,L. Chioncel, A. I. Lichtenstein and R. A. de Groot, Rev. Mod. Physics **80**, 318, (2008).

[34] S. A. Hatfield and G. R. Bell, Surf. Sci. **61**, 5368 (2007).

[35] S. A. Hatfield, J. D. Aldous, and G. R. Bell, Appl. Surf. Sci. **225**, 3567 (2009).

[36] M. Grundmann, Phys. Stat. Sol. B **248**, 805 (2011).

[37] S. Mollet and S. J. Jenkins, J. Phys. Condens. Matt. **19**, 315214 (2007).

[38] S. J. Jenkins, Phys. Rev. B Rapid Comm. **82**, 020403 (2010).